

Reduced mitochondrial respiration in hybrid asexual lizards

Supplementary Materials

Randy L. Klabacka^{1,*}, Hailey A. Parry¹, Kang N. Yap¹, Ryan A. Cook^{1,2}, Victoria A. Herron^{1,3},
L. Miles Horne^{1,4}, Matthew E. Wolak¹ Jose A. Maldonado⁵, Andreas N. Kavazis¹, Matthew K. Fujita⁵,
Jamie R. Oaks^{1,†}, Tonia S. Schwartz^{1,†}

1. Auburn University, Auburn, AL 36849;
 2. Villanova University, Villanova, PA, 19085;
 3. University of Missouri College of Veterinary Medicine, Columbia, MO, 65211
 4. The University of Texas at El Paso, El Paso, TX, 79968;
 5. The University of Texas at Arlington, Arlington, TX, 76019;
- * Corresponding author; e-mail: klabacka.randy@auburn.edu.
† These authors contributed equally to the manuscript

Journal: American Naturalist

Manuscript type: Note.

Supplementary Methods

Animal Capture

We collected individuals along the Rio Grande basin between Las Cruces, New Mexico and Big Bend National Park, Texas. We caught thirty lizards (Table S1) either via lasso or by hand, and transported all individuals to Auburn University for temporary housing. Lizards were housed in laboratory conditions reflecting their typical desert habitat (25° C burrowing conditions, 40° C sunning conditions), and were fed ad libitum (crickets and mealworms) and watered daily (Townsend 1979). Individuals were accessioned as alcohol-preserved specimens in the Auburn University Museum of Natural History.

Endurance Capacity

After one month of acclimation to lab conditions, we randomly ordered individuals for treadmill running. After fasting the lizards 24 hours, we measured endurance capacity by timing the number of seconds an individual maintained forward progression on a treadmill moving at 1 km/hr (measured with a stopwatch). We terminated each trial when an individual could no longer keep pace with the treadmill following five repeated prompts (light pinching at base of tail). We log (Log_{10}) transformed the endurance measurement for all statistical models including endurance following visual inspection of the distribution of residuals (log transformation showed a more normal distribution of residuals). For all models comparing the effect of reproductive mode on endurance, we included snout-vent length (SVL) as a covariate for body size (Garland, 1994).

Mitochondrial Isolation and Respirometry

One week after endurance trials, we randomly ordered individuals and assigned them to days for live mitochondrial respirometry. After fasting lizards one day, we euthanized animals via decapitation and immediately excised and transferred skeletal muscle from the front and hind limbs to 10 w/v of isolation buffer (100 mM l⁻¹ KCl, 40 mM l⁻¹ Tris-HCl, 10 mM l⁻¹ Tris base, 1 mM l⁻¹ MgCl₂, 1 mM l⁻¹ EGTA, 0.2 mM l⁻¹ ATP and 0.15 percent [w/v] free fatty acid bovine serum albumin [BSA], pH 7.50). After mincing muscle tissue, we homogenized the sample with VITRIS-5 homogenizer at medium power for five seconds and added fresh protease (Trypsin-T1426: 5 mg/g wet muscle). Homogenate was then mixed every 30 seconds for seven minutes before digestion was terminated with an equal volume of isolation

buffer. We then centrifuged the sample at 500 xG for 10 minutes at 4°C, and passed the supernatant through gauze. We performed two steps of centrifugation at 4969 xG for 15 minutes at 4° C, with resuspension of the mitochondrial pellet following each of these two centrifugations (using isolation buffer with a volume equal to that of the original isolation buffer used, but the second resuspension used isolation buffer lacking BSA). Following centrifugation, we suspended the final mitochondrial pellet in 100 µl mannitol/sucrose solution (220 mmol l⁻¹ mannitol, 70 mmol l⁻¹ sucrose, 10 mmol l⁻¹ Tris-HCl, and 1 mmol l⁻¹ EGTA; pH 7.40).

We added isolated mitochondria to respiration buffer (100 mM KCl, 10 mM KH₂PO₄, 1 mM EGTA, 50 mM MOPS, 10 mM MgCl₂, 20 mM glucose, and 0.2 percent BSA) in two water-jacketed respiratory chambers (Hansatech Oxytherm; hereafter referred to as chambers A and B) with continuous stirring at 40°C . We measured respiration by quantifying oxygen consumption with 2 mM pyruvate, 2 mM malate and 10 mM glutamate substrates in chamber A for respiration initiated through complex I (CI), and 5 mM succinate as a substrate with 5 µM of rotenone to inhibit CI in chamber B for respiration initiated through complex II (CII). We began ADP-stimulated respiration (State 3) by adding 0.25 mM ADP in each chamber. Basal respiration (State 4), which occurs when oxygen consumption is driven by protons "leaking" across the inner membrane, was recorded after the phosphorylation of ADP was complete. Respiration rates were normalized to mitochondrial protein content determined via Bradford assay. Respiratory control ratio (RCR) was calculated by dividing state 3 respiration by state 4 respiration. Mitochondria isolation and respirometry were both executed in a manner where the researchers and data recorders were blind to the species and mode of reproduction.

Phylogenetic Network Estimation

We sequenced mitochondrial genomes following methods described by (Roelke et al., 2015) and downloaded available mitochondrial sequence data from GenBank for phylogenetic estimation (Table S2). We aligned sequences using the MAFFT v7.388 algorithm (Katoh et al., 2002) within the sequence editing program Geneious Prime v2019.0.4. We bootstrapped the sequence alignment (1000 nonparametric replicates), estimated the maximum likelihood tree for each bootstrap replicate, and used the maximum likelihood trees (with the -m TEST command to perform standard model selection) to construct a consensus tree using the program IQ-Tree (Nguyen et al., 2015; see Fig S1). We pruned the tree to include only the focal taxa for this study using the R package ape. Because this gene tree only represented the maternal mitochondrial ancestry, to approximate the paternal history we pruned copies

of the asexual hybrid lineages from their maternal sister lineage and grafted these in with their paternal sister lineage while preserving the branch lengths. The reticulation at the base of an asexual lineage occurs at the hybridization event between two sexual species. Shortly after this event, the asexual species' mitochondrial gene tree (which generally sorts [coalesces] faster than the nuclear ancestry due to the smaller effective population size) diverged from the maternal sexual ancestor, providing an upper bound on the time of hybridization. While using this paternal tree would not be an appropriate reference for understanding the evolution of the nuclear genome in the hybrid lineages, it is adequate to reconstruct the reticulate phylogeny that is currently supported from previous studies with these species (Densmore et al., 1989). With the maternal and paternal trees as input, we estimated the phylogenetic network using the InferNetwork_ML (maximum likelihood) command in the program PhyloNet (Than and Nakhleh, 2008; see Fig S1).

Linear Modeling and Analyses

We analyze the data in three ways.

Phylogenetic Linear Models

First, in order to account for reticulate evolutionary history, we constructed phylogenetic network linear models to test (1) the effect of hybrid asexuality on each response variable (Log_{10} Endurance, CI State 3, CI State 4, CI RCR, CII State 3, CII State 4, and CII RCR) and (2) the effect of mitochondrial respiration on endurance capacity using the function phylolm within the Julia package PhyloNetworks (Solis-Lemus et al., 2017) . These models included the phylogenetic network to compute the variance matrix for the linear regression. Within-species variation was captured using the `y_mean_std` flag to incorporate standard deviation into the model.

Linear Mixed-Effects Models

Second, we designed linear mixed-effects models with species random effects to again test for (1) an effect of hybrid asexuality on each response variable, (2) differences in variation between hybrid asexual and sexual species for each response variable, and (3) the effect of mitochondrial respiration on endurance capacity. In this approach we did not include phylogenetic relatedness, therefore all species are independent. We created linear models using the R packages nlme and MCMCglmm. Here we briefly describe the model architecture; model specifics can be seen in the annotated code file

StatisticalAnalysis.R. Results from the analyses are shown in Table S5.

For each response variable, we created two linear models using the function lme: (1) a model with the sexual mode as a fixed-effect independent variable and species as a random variable and (2) a model with the same components as model 1, with an additional residual variation parameter [allowing for different variability for sexual and hybrid asexual species]. We fit the models to the data and performed a likelihood ratio test to compare model fit (to test whether a model with two parameters of variation fit better than a model with a single parameter). For the models including two residual variation parameters, we obtained estimates of uncertainty by performing nonparametric bootstrapping (1000 replicates) and re-estimating the standard deviation.

Because there can be a linear relationship between the mean and variance on the scale of measurement, estimates of variance using mean-corrected approaches can provide a conservative approach to assessing heteroscedasticity. To account for the possibility that differences in variance between sexual and asexual species is due to differences in scale of the response variable, we also used a Bayesian approach to compare mean-corrected standard deviations. Within models constructed using MCMCglmm, we used a non-informative prior, a burn-in of 3000, a thinning interval of 50, and a chain length of 53,000 (giving us 1,000 samples of the posterior). Each model contained unique residual variance parameters for each of the reproductive modes to allow for differences in variance between sexual and hybrid asexual species (Fig S3). For each MCMC sample, we calculated the difference between hybrid asexual and sexual species in the coefficient of variation (i.e., the standard deviation divided by the mean). We then compared the coefficients of variation between reproductive modes by subtracting the posterior distribution of the hybrid asexual species from that of the sexual species (Fig S4).

Subgroup Linear Models

Third, in order to examine the same effects we described in the linear mixed-effects model within individual subgroups (i.e., without needing to account for ancestry), we constructed linear models for (A) the *tesselatus* and *neomexicanus* groups independently (comparing each hybrid asexual to its parental species) and (B) all species with the same mitochondrial ancestry (*Aspidoscelis marmoratus*, *A. neomexicanus*, and *A. tesselatus*). While ideally the latter would include information regarding which of the two asexual groups first arose, such information is yet to be estimated (thus we assume they arose at the same time).

Supplementary Results

Within-group ANOVAs

We observed the same general pattern in the *Tesselatus* and *Neomexicanus* groups (reduced endurance and respiration [State 3 and 4] in hybrid asexual species compared to parental sexual species), however, many of the models were not statistically significant (Table S4). RCR for both CI and CII showed no differences between sexual parents and hybrid asexuals. The models including the three species with similar mitochondrial haplotypes (*Aspidoscelis marmoratus*, *A. neomexicanus*, *A. tesselatus*) showed reduced endurance and maximal and basal respiration (State 3 and 4 for CI and CII) of both hybrid asexuals compared to *A. marmoratus*, although models for CI State 4 and CII State 4 were not statistically significant (Table S4). RCR for both CI and CII showed no differences between *A. marmoratus* and hybrid asexuals.

Study Limitations

Ideally our sampling would have focused entirely on female individuals and been larger than 30 individuals per species. Although we aimed to collect only female individuals, challenges of capturing sufficient females within our timeframe led to our inclusion of males in the dataset (the lizards within this study system are particularly difficult to capture). We found this justifiable based on previous work showing marginal sexual dimorphism within the same species examined in this study (Cullum, 1998), and on this basis we determined that bias due to sex would be minor. Although removing males severely reduces our sample size and dramatically decreases the power for our analyses, when we perform analyses in a female-only dataset we see that the direction of the patterns remain consistent with our conclusions.

Because post-hoc tests can impose an unnecessarily strict procedure to an underpowered dataset (Nakagawa, 2004), we do not perform post-hoc corrective tests. We recognize the possible contribution of false positives within our results and encourage replication.

References Cited Only in the Online Enhancements

Literature Cited

- Cullum, A. J. , 1998. Sexual dimorphism in physiological performance of whiptail lizards (genus *cnemidophorus*). *Physiological Zoology* 71:541–552.
- Katoh, K., K. Misaawa, K. Kuma, and T. Miyata. , 2002. Mafft: a novel method for rapid multiple sequence alignment based on fast fourier transform. *Nucleic Acids Research* 30:3059–3066.
- Nakagawa, S. , 2004. A farewell to bonferroni: the problems of low statistical power and publication bias. *Behavioral Ecology* 15:1044–1045.
- Solis-Lemus, C., P. Bastide, and C. Ane. , 2017. Phylonetworks: A package for phylogenetic networks. *Molecular Biology and Evolution* 34.

Supplementary Tables and Figures

Table S1 Sample information.

Table S2 List of individuals used for phylogenetic inference.

Table S3 Summary statistics

Table S4 Within-group linear models

Table S4 Differences in variance between sexual and hybrid asexual species

Figure S1 Evolutionary relationships

Figure S2 Endurance and mitochondrial respiration of sexual and hybrid asexual species

Figure S3 Standard deviations for sexual and hybrid asexual species

Figure S4 Posterior distributions of coefficient of variation

Table S1: Sample Information

Field ID	Species	Capture Date	State	County	Lat	Long	Endurance		CI RCR		CII State 4		CII RCR			
							CI State 3	CI State 4	CI State 4	CI State 3	CII State 3	CII State 4	CI RCR	CII RCR		
RLK178	<i>A. inornatus</i>	5/16/2019	sex	4.9	M	TX	Brewster	29.3024	-103.1735	3.47	24.17	6.43	3.76	22.80	13.52	1.69
RLK198	<i>A. inornatus</i>	5/24/2019	sex	5.3	M	TX	Hudspeth	30.776757	-105.016495	12.37	28.38	9.12	3.11	28.19	15.72	1.79
RLK200	<i>A. inornatus</i>	5/25/2019	sex	5.1	F	TX	Hudspeth	30.777342	-105.016564	4.03	21.14	3.83	5.52	18.84	8.19	2.30
RLK204	<i>A. inornatus</i>	5/26/2019	sex	5.8	M	TX	Hudspeth	30.776901	-105.016291	9.17	30.09	8.8	3.42	21.76	13.41	1.62
RLK210	<i>A. inornatus</i>	5/29/2019	sex	5.5	M	NM	Doña Ana	32.249198	-106.821715	4.62	23.23	7.04	3.30	21.59	11.17	1.93
RLK211	<i>A. inornatus</i>	5/29/2019	sex	5.6	M	NM	Doña Ana	32.249134	-106.82207	12.05	33.35	10.36	3.22	33.71	17.71	1.90
RLK186	<i>A. marmoratus</i>	5/18/2019	sex	8.2	M	TX	Brewster	29.1775	-102.9989	5.68	29.83	12.81	2.33	28.61	18.23	1.57
RLK187	<i>A. marmoratus</i>	5/18/2019	sex	6.9	M	TX	Brewster	29.1781	-102.9977	5.38	30.11	8.57	3.51	27.80	15.01	1.85
RLK191	<i>A. marmoratus</i>	5/19/2019	sex	7.8	F	TX	Brewster	29.1781	-102.9974	6.55	22.85	4.8	4.76	19.74	6.36	3.11
RLK193	<i>A. marmoratus</i>	5/19/2019	sex	7.4	M	TX	Brewster	29.1781	-102.9974	5.50	25.01	7.29	3.43	23.52	10.91	2.16
RLK205	<i>A. marmoratus</i>	5/25/2019	sex	8.6	M	TX	Hudspeth	30.775838	-105.015899	6.07	21.36	6.01	3.55	20.08	9.03	2.22
RLK206	<i>A. marmoratus</i>	5/28/2019	sex	8.7	M	NM	Doña Ana	32.25602	-107.63207	8.42	29.70	7.99	3.72	26.08	12.29	2.12
RLK208	<i>A. neomexicanus</i>	5/28/2019	asex	5.7	F	NM	Doña Ana	32.24994	-106.82133	2.50	15.49	5.82	2.66	15.54	8.73	1.78
RLK212	<i>A. neomexicanus</i>	5/29/2019	asex	6.9	F	NM	Doña Ana	32.24704	-106.82327	3.13	20.93	6.35	3.30	20.26	9.53	2.13
RLK213	<i>A. neomexicanus</i>	5/29/2019	asex	6.1	F	NM	Doña Ana	32.24631	-106.82299	3.83	26.48	6.36	4.16	21.72	11.32	1.92
RLK214	<i>A. neomexicanus</i>	5/30/2019	asex	6.7	F	NM	Doña Ana	32.25612	-106.84009	4.45	15.24	4.01	3.80	22.81	10.40	2.19
RLK165	<i>A. septentrionalis</i>	5/15/2019	sex	9.1	M	TX	Brewster	29.2589	-103.2987	4.80	20.71	5.79	3.58	21.03	12.03	1.75
RLK170	<i>A. septentrionalis</i>	5/15/2019	sex	8.5	M	TX	Brewster	29.254819	-103.300742	7.65	20.50	6.82	3.01	21.58	13.11	1.65
RLK171	<i>A. septentrionalis</i>	5/15/2019	sex	8.2	M	TX	Brewster	29.260019	-103.297041	7.10	34.62	10.61	3.26	33.57	16.51	2.03
RLK172	<i>A. septentrionalis</i>	5/15/2019	sex	8.5	F	TX	Brewster	29.259492	-103.297782	15.85	35.46	10.13	3.50	30.08	15.54	1.94
RLK174	<i>A. septentrionalis</i>	5/16/2019	sex	7.0	F	TX	Brewster	29.2959	-103.1771	4.07	25.87	7.41	3.49	27.21	13.88	1.96
RLK176	<i>A. septentrionalis</i>	5/16/2019	sex	7.2	M	TX	Brewster	29.29646	-103.17565	4.50	28.16	10.7	2.63	26.18	16.14	1.62
RLK177	<i>A. septentrionalis</i>	5/16/2019	sex	7.7	F	TX	Brewster	29.3024	-103.1735	8.47	30.11	8.53	3.53	21.90	9.53	2.30

Table S1: Sample Information (cont.)

Field ID	Species	Capture Date	Reprod	SVL	Sex	State	County	Lat	Long	Endurance	CI State 3	CI State 4	CI RCR	CII State 3	CII State 4	CII RCR
RLK162	<i>A. tesselatus</i>	5/15/2019	asex	8.1	F	TX	Brewster	29.324813	-104.035785	3.73	24.75	6.14	4.03	20.78	10.21	2.04
RLK181	<i>A. tesselatus</i>	5/17/2019	asex	7.7	F	TX	Brewster	29.1622	-103.6143	2.95	20.38	5.18	3.93	21.02	12.88	1.63
RLK182	<i>A. tesselatus</i>	5/17/2019	asex	6.6	F	TX	Brewster	29.3055	-103.1781	3.98	15.34	6.41	2.39	15.83	10.02	1.58
RLK183	<i>A. tesselatus</i>	5/17/2019	asex	7.2	F	TX	Brewster	29.3055	-103.1743	3.13	27.56	5.06	5.45	18.90	8.42	2.25
RLK185	<i>A. tesselatus</i>	5/18/2019	asex	7.8	F	TX	Brewster	29.1775	-102.9989	5.27	18.42	5.86	3.14	16.75	8.98	1.87
RLK189	<i>A. tesselatus</i>	5/18/2019	asex	6.5	F	TX	Brewster	29.1779	-102.9981	4.02	18.74	5.62	3.34	16.95	8.62	1.97
RLK194	<i>A. tesselatus</i>	5/19/2019	asex	8.6	F	TX	Brewster	29.177572	-102.997929	4.82	16.55	6.37	2.60	19.05	9.72	1.96

Table S2: Individuals used for phylogenetic inference

GenBank Accession	Species	Loci	Field ID
OK104662	<i>Aspidoscelis gularis</i>	MtDNA Genome	ASH22
OK104663	<i>Aspidoscelis gularis</i>	MtDNA Genome	ASH25
OK104664	<i>Aspidoscelis gularis</i>	MtDNA Genome	ASH63
AY620808.1	<i>Aspidoscelis inornatus</i>	ND4	NA
AY620811.1	<i>Aspidoscelis inornatus</i>	ND4	NA
AY620813.1	<i>Aspidoscelis inornatus</i>	ND4	NA
AY620812.1	<i>Aspidoscelis inornatus</i>	ND4	NA
OK104676	<i>Aspidoscelis inornatus</i>	MtDNA Genome	ASH120
OK104677	<i>Aspidoscelis inornatus</i>	MtDNA Genome	ASH121
MZ673806	<i>Aspidoscelis inornatus</i>	MtDNA Genome	ASH124
OK104678	<i>Aspidoscelis inornatus</i>	MtDNA Genome	ASH123
OK104715	<i>Aspidoscelis sexlineatus</i>	MtDNA Genome	KLC154
OK104716	<i>Aspidoscelis sexlineatus</i>	MtDNA Genome	KLC156
OK104717	<i>Aspidoscelis sexlineatus</i>	MtDNA Genome	KLC157
OK104681	<i>Aspidoscelis marmoratus</i>	MtDNA Genome	ASH131
OK104685	<i>Aspidoscelis marmoratus</i>	MtDNA Genome	ASH145
OK104686	<i>Aspidoscelis marmoratus</i>	MtDNA Genome	ASH146
OK104730	<i>Aspidoscelis neomexicanus</i>	MtDNA Genome	RLK89
OK104731	<i>Aspidoscelis neomexicanus</i>	MtDNA Genome	RLK90
OK104668	<i>Aspidoscelis tesselatus</i>	MtDNA Genome	ASH80
OK104669	<i>Aspidoscelis tesselatus</i>	MtDNA Genome	ASH97
OK104665	<i>Aspidoscelis tesselatus</i>	MtDNA Genome	ASH70
OK104670	<i>Aspidoscelis tesselatus</i>	MtDNA Genome	ASH98
OK104687	<i>Aspidoscelis marmoratus</i>	MtDNA Genome	ASH148
AF026179.1	<i>Aspidoscelis septemvittatus</i>	ND4	NA
AF026181.1	<i>Aspidoscelis septemvittatus</i>	ND4	NA
AF026182.1	<i>Aspidoscelis septemvittatus</i>	ND4	NA
AF026170	<i>Teius teyou</i>	ND4	NA
AF151207	<i>Kentropyx viridistriga</i>	ND4	NA

Table S3: Summary statistics for species and reproductive modes

	Species					Repro Mode	
	<i>A. inornatus</i>	<i>A. marmoratus</i>	<i>A. neomexicanus</i>	<i>A. septemvittatus</i>	<i>A. tesselatus</i>	Hybrid Asexual	Sexual
Endurance							
\bar{x}	7.62	6.27	3.48	7.49	3.99	3.80	7.14
σ	4.09	1.14	0.85	4.06	0.84	0.84	3.30
95% CI	$\bar{x} \pm 1.67$	$\bar{x} \pm 0.46$	$\bar{x} \pm 0.42$	$\bar{x} \pm 1.53$	$\bar{x} \pm 0.32$	$\bar{x} \pm 0.25$	$\bar{x} \pm 0.76$
CI State 3							
\bar{x}	26.73	26.48	19.54	27.92	20.25	20.00	27.09
σ	4.65	3.91	5.32	6.03	4.42	4.51	4.77
95% CI	$\bar{x} \pm 1.90$	$\bar{x} \pm 1.59$	$\bar{x} \pm 2.66$	$\bar{x} \pm 1.28$	$\bar{x} \pm 1.67$	$\bar{x} \pm 1.36$	$\bar{x} \pm 1.09$
CI State 4							
\bar{x}	7.60	7.91	5.64	8.57	5.81	5.74	8.05
σ	2.34	2.76	1.11	1.97	0.55	0.75	2.26
95% CI	$\bar{x} \pm 0.95$	$\bar{x} \pm 1.13$	$\bar{x} \pm 0.556$	$\bar{x} \pm 0.744$	$\bar{x} \pm 0.21$	$\bar{x} \pm 0.23$	$\bar{x} \pm 0.52$
CI RCR							
\bar{x}	3.72	3.55	3.48	3.29	3.55	3.53	3.51
σ	0.91	0.77	0.65	0.35	1.04	0.88	0.69
95% CI	$\bar{x} \pm 0.37$	$\bar{x} \pm 0.32$	$\bar{x} \pm 0.33$	$\bar{x} \pm 0.13$	$\bar{x} \pm 0.39$	$\bar{x} \pm 0.27$	$\bar{x} \pm 0.16$
CII State 3							
\bar{x}	24.48	24.31	20.08	25.94	18.47	19.06	24.96
σ	5.47	3.83	3.20	4.77	2.02	2.49	4.53
95% CI	$\bar{x} \pm 2.23$	$\bar{x} \pm 1.56$	$\bar{x} \pm 1.60$	$\bar{x} \pm 1.80$	$\bar{x} \pm 0.77$	$\bar{x} \pm 0.75$	$\bar{x} \pm 1.04$
CII State 4							
\bar{x}	13.29	11.97	10.00	13.82	9.84	9.89	13.07
σ	3.35	4.24	1.12	2.51	1.51	1.32	3.29
95% CI	$\bar{x} \pm 1.37$	$\bar{x} \pm 1.73$	$\bar{x} \pm 0.56$	$\bar{x} \pm 0.95$	$\bar{x} \pm 0.57$	$\bar{x} \pm 0.40$	$\bar{x} \pm 0.75$
CII RCR							
\bar{x}	1.87	2.17	2.00	1.89	1.90	1.94	1.97
σ	0.24	0.52	0.19	0.24	0.23	0.21	0.36
95% CI	$\bar{x} \pm 0.10$	$\bar{x} \pm 0.21$	$\bar{x} \pm 0.10$	$\bar{x} \pm 0.09$	$\bar{x} \pm 0.09$	$\bar{x} \pm 0.06$	$\bar{x} \pm 0.08$

\bar{x} = mean, σ = standard deviation. Endurance is time in minutes. Respiration states are nmoles O₂ consumed per minute per mg of protein.

Table S4: Within-group linear models

	tess model	tess-marm	tess-sept	neom model	neom-marm	neom-inor	marm model	neom-marm	tess-marm	
Log₁₀ Endur										
	β	NA	-0.17	-0.20	NA	-0.043	-0.43	NA	-0.17	-0.18
	SE	NA	0.076	0.074	NA	0.16	0.13	NA	0.074	0.11
	p	0.011	0.041	0.016	0.032	0.80	0.0060	8.60E-04	0.034	0.0031
CI State 3										
	β	NA	-6.23	-7.67	NA	-6.94	-7.19	NA	-6.94	-6.23
	SE	NA	2.74	2.63	NA	2.94	2.94	NA	2.88	2.48
	p	0.023	0.036	0.0096	0.056	0.034	0.024	0.039	0.030	0.025
CI State 4										
	β	NA	-2.11	-2.76	NA	-2.28	-1.96	NA	-2.28	-2.11
	SE	NA	1.07	1.03	NA	1.49	1.49	NA	1.14	0.98
	p	0.041	0.066	0.016	0.31	0.15	0.21	0.086	0.066	0.050
CI RCR										
	β	NA	-0.0044	0.27	NA	-0.070	-0.24	NA	-0.070	-0.0044
	SE	NA	0.43	0.41	NA	0.52	0.52	NA	0.56	0.49
	p	0.77	0.99	0.52	0.88	0.90	0.65	0.99	0.90	0.99
CII State 3										
	β	NA	-5.84	-7.47	NA	-4.22	-4.40	NA	-4.22	-5.84
	SE	NA	2.07	1.98	NA	2.85	2.85	NA	1.96	1.69
	p	0.0040	0.012	0.0016	0.28	0.16	0.15	0.012	0.049	0.0038
CII State 4										
	β	NA	-2.14	-3.98	NA	-1.98	-3.29	NA	-1.98	-2.14
	SE	NA	1.60	1.54	NA	2.19	2.19	NA	1.79	1.54
	p	0.059	0.20	0.019	0.35	0.38	0.16	0.36	0.29	0.19
CII RCR										
	β	NA	-0.28	0.0061	NA	0.13	-0.17	NA	-0.17	-0.27
	SE	NA	0.19	0.18	NA	0.24	0.24	NA	0.23	0.20
	p	0.28	0.17	0.97	0.39	0.59	0.49	0.41	0.48	0.19

Effect sizes (β), standard error (SE), and p-values (p) for each response variable. The tess model (left) includes effects between maternal-hybrid (tess-marm) and paternal-hybrid (tess-sept). The neom model (center) includes effects between maternal-hybrid (neom-marm) and paternal-hybrid (neom-sept). The marm model (right) includes effects between hybrids and the maternal offspring (neom-marm and tess-marm). We considered effects with $p < 0.05$ as statistically significant.

Table S5: Differences in variance between sexual and hybrid asexual species

	lme				MCMCglmm			
	$\sigma s, \sigma a$	SEs, SEa	L Ratio	p	$\sigma s, \sigma a$	(95% HPDs), (95% HPDa)	ΔCV	P
Endurance	0.18,0.090	0.030,0.016	5.19	0.023	0.20,0.11	(0.13-0.26),(0.067-0.18)	0.027	0.75
CI State 3	4.77,4.51	0.56,0.84	0.041	0.84	5.27,5.29	(3.38-7.20),(3.09-8.34)	-0.076	0.21
CI State 4	2.26,0.75	0.36,0.19	11.44	7e-04	2.47,0.89	(1.63-3.43),(0.512-1.37)	0.14	0.96
CI RCR	0.69,0.88	0.17,0.21	0.81	0.37	0.75,0.103	(0.49-1.02),(0.59-1.63)	-0.08	0.20
CII State 3	4.53,2.49	0.62,0.48	3.95	0.047	4.95,2.86	(3.469-6.89),(1.63-4.39)	0.069	0.83
CII State 4	3.29,1.32	0.51,0.36	8.28	0.004	3.55,1.58	(2.55-4.99),(0.90-2.48)	0.11	0.94
CII RCR	0.36,0.21	0.084,0.039	8.55	0.088	0.38,0.25	(0.26-0.52),(0.14-0.38)	0.063	0.89

LME SECTION: Standard deviations for the lme model fitting two residual variation parameters to the data (for the reproductive modes) are shown under $\sigma s, \sigma a$ (standard deviation for sexual species, hybrid asexual species). The standard errors for each reproductive mode (SEs, SEa) were estimated using a nonparametric bootstrap approach. For each response variable, a likelihood ratio test was performed between a model fitting a single residual variation parameters and a model fitting two residual variation parameters (for the reproductive modes). L Ratio is the likelihood ratio score. p is the p-value for the likelihood ratio test, with $p < 0.05$ indicating the model with two residual variation parameters is a better fit for the data. MCMCglmm SECTION: Standard deviations determined by calculating the mean of the posterior distribution for the MCMCglmm model fitting two residual variance parameters to the data (for the reproductive modes) are shown under $\sigma s, \sigma a$ (standard deviation for sexual species, hybrid asexual species). (95% HPDs), (95% HPDa) is the 95% credible interval for the standard deviations estimated from the posterior distribution (see Fig S3 for a posterior distribution of the standard deviations estimated from the MCMCglm approach). ΔCV is the mean difference for the coefficient of variation (sexual - asexual hybrid). P is the posterior probability that the sexual coefficient of variation is greater than the hybrid asexual coefficient of variation Fig S4.

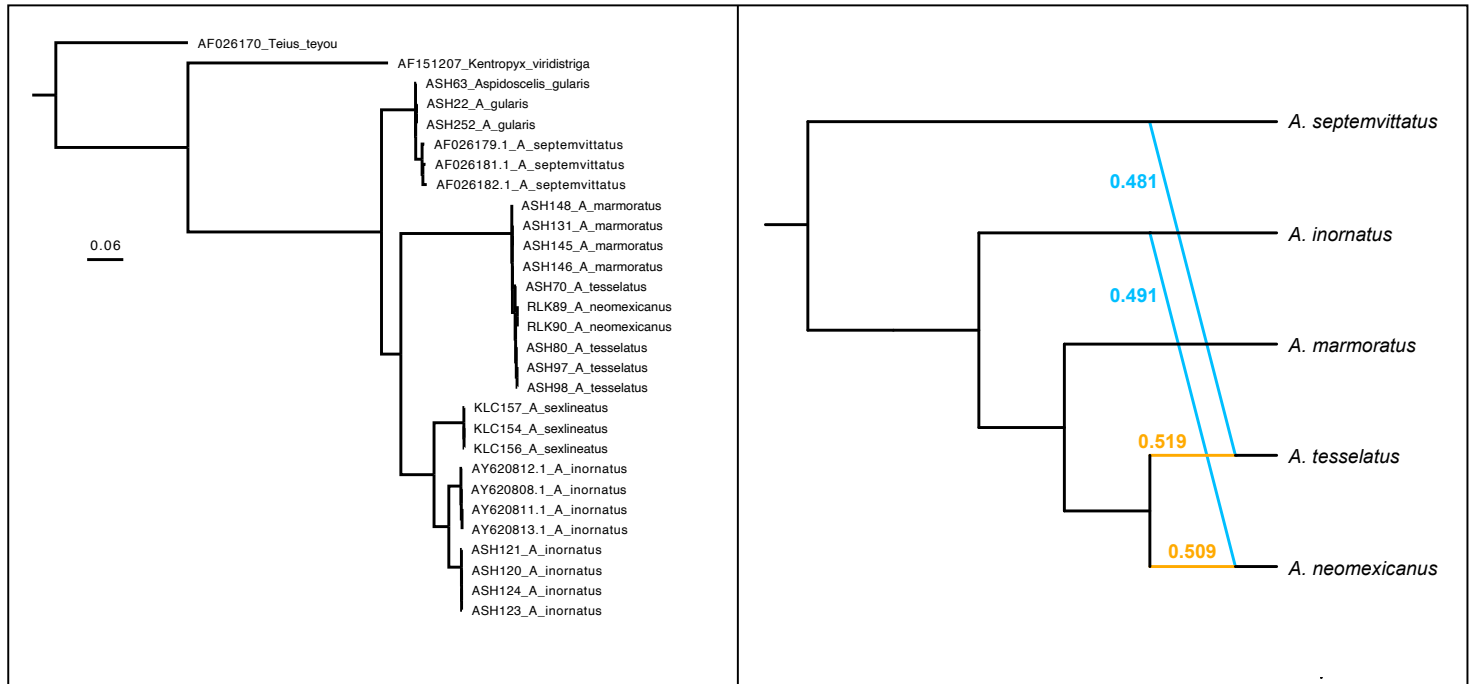


Figure S1: Left: mitochondrial consensus tree constructed from 1000 bootstrap replicates of the mitochondrial alignment with subsequent maximum likelihood tree estimation using IQ-Tree with individuals described in Table S3. Right: Phylogenetic network estimated using PhyloNet using mitochondrial relationships from the mitochondrial consensus tree and an estimated paternal ancestry. Blue lines represent estimated contribution from paternal ancestor, and yellow lines represent estimated contribution from maternal ancestor.

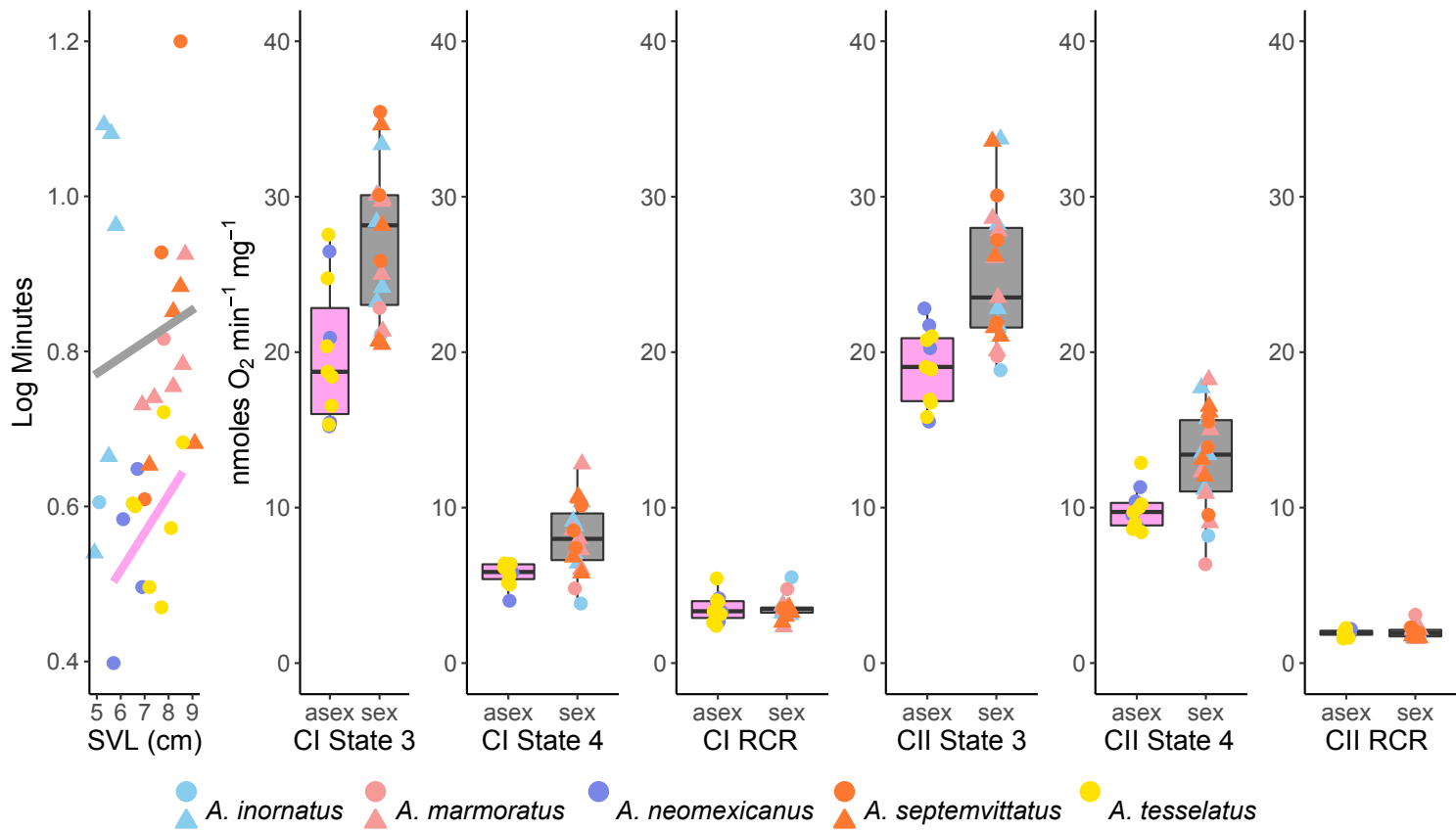


Figure S2: Plots showing effect of hybrid asexuality on mitochondrial respiration. Each plot corresponds to the individual data from Table S1. All models showed a significant difference between sexual and hybrid asexuals for the response variables for both lme and phylonetwoklm approaches ($p < 0.05$) except for the two models for RCR. Point symbols represent males (triangles) and females (circles)

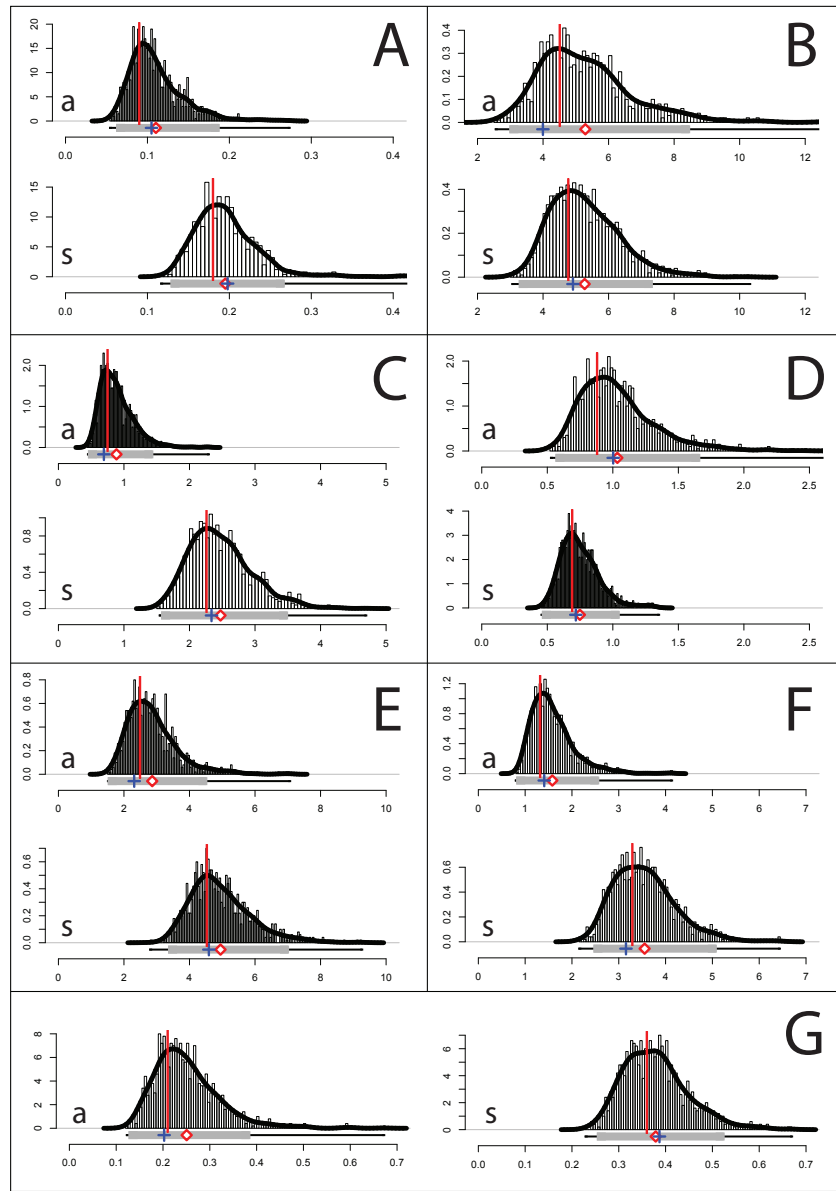


Figure S3: Plots showing the approximate posterior distribution for the standard deviation for sexual (s) and hybrid asexual (a) species for each of the response variables: (A) Endurance, (B) CI State 3 Respiration, (C) CI State 4 Respiration, (D) CI RCR, (E) CII State 3 Respiration, (F) CII State 4 Respiration, and (G) CII RCR. Posteriors distributions were estimated using the MCMCglmm package in R. The gray bar on the x-axis is the 95% credible interval, with the red diamond and blue cross marking the mean and mode, respectively. The red line marks the standard deviation estimated from the nlme::lme approach.

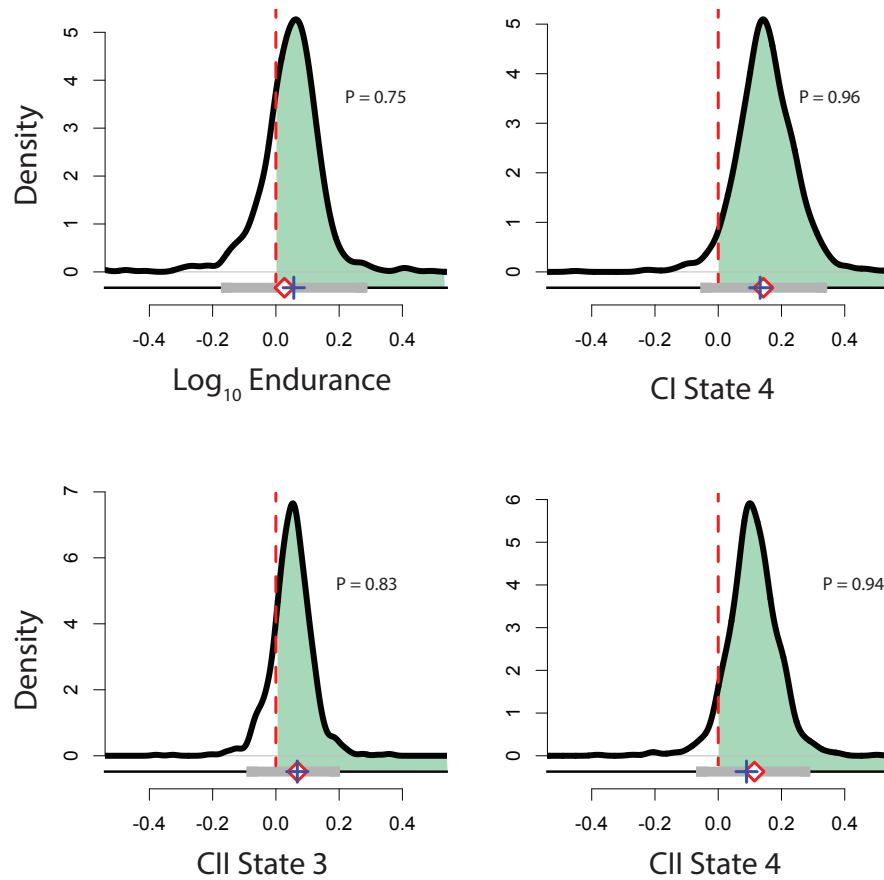


Figure S4: Plots showing the approximate posterior distribution for the sexual-asequel difference between coefficient of variance posterior distributions. The gray bar on the x-axis is the 95% credible interval, with the red diamond and blue cross marking the mean and mode, respectively. P = posterior probability that the sexual coefficient of variation is greater than the asexual coefficient of variation. The dashed red line marks the line where the sexual and asexual coefficient of variations are equal, with the green area under the curve showing the area of the posterior distribution with greater coefficient of variation in sexual species compared to hybrid asexual species.